Role of macroporosity in runoff generation on a sloping subsurface drained clay field — a case study with MACRO model

Salka Hintikka, Harri Koivusalo, Maija Paasonen-Kivekäs, Visa Nuutinen and Laura Alakukku

ABSTRACT

Macroporosity and its effect on runoff processes were studied on a sloping subdrained clay field (very fine Aeric Cryaquept) in Southern Finland. An extensive field campaign was carried out to measure the spatial variability of soil macroporosity and hydraulic properties. According to the field data, macropore conductivity decreased with depth and soil properties showed differences between the upper and lower parts of the field. A one-dimensional model (MACRO) was applied to quantify the effect of these differences on the hydrological response of the upper and lower field sites. Based on the measurements, five separate parameterizations characterizing the differences in soil structure between the measurement sites were formulated. The change in soil structure had a great effect on the relative proportions of simulated drain flow and surface runoff but influenced only slightly the total amount of runoff. Evapotranspiration and percolation were similar in all cases. Examining model simulations, measured runoff components and groundwater table suggested that a two- or three-dimensional modeling approach is necessary, when prediction of proportional fractions of drain flow and surface runoff, and simulation of groundwater level in a sloping field are of interest.

Key words | clay, drain flow, macropores, modelling, surface runoff

Salka Hintikka
Maija Paasonen-Kivekäs
Harri Koivusalo (corresponding author)*
Laboratory of Water Resources Engineering,
Helsinki University of Technology,
PO Box 5200, FI-02015 TKK,
Finland
*Finnish Forest Research Institute,
Joensuu Research Unit,
PO Box 68, FI-80101 Joensuu,
Finland
Tel.: +358 50391 3112
E-mail: *Harri.Koivusalo@metla.fi*

Visa Nuutinen
Laura Alakukku†
MTT Agrifood Research Finland,
FI-31600 Jokioinen,
Finland
†Department of Agrotechnology,
University of Helsinki,
PO Box 28, FI-00014 Helsinki,
Finland

INTRODUCTION

Water and nutrients from agricultural fields are transported to lakes and rivers with surface runoff and drain flow. Surface runoff and erosion contribute heavily to losses of agrochemicals adsorbed on soil particles, whereas water-soluble nutrients and pesticides are prone to leach through the vadose zone into groundwater and subsurface drains. Occurrence of preferential flow in soil can significantly increase transport through subsurface drains (e.g. Paasonen-Kivekas *et al.* 2000; Jaynes *et al.* 2001; Fox *et al.* 2004). Especially on heavy textured soils drain flow consists mostly of preferential flow, i.e. water that has bypassed the soil matrix through a network of macropores and cracks (Villhoth *et al.* 1998; Heppel *et al.* 2000). As water has less time to be in contact with the soil aggregates fertilisers and pesticides may leach into the drains or the deep groundwater zone instead of being adsorbed on the surface of soil aggregates.

Macropores usually occupy a small proportion of the entire soil porosity (see, for example, Aura 1990; Alakukku 1998; Jarvis 2007) and contribute to flow only over a short period of time during and after a rainfall or snowmelt event. Macropore flow capacity, however, may exceed that of the soil matrix by several orders of magnitude and, in certain soils, macropores dominate both infiltration and soil water flow (Watson & Luxmoore 1986; Mitchell & van Genuchten 1993; Novak *et al.* 2000). Quantifying volume and structure of macropores is problematic due to their great spatial and temporal variability. Even though total macroporosity and its flow capacity can be determined, for example, with tension

doi: 10.2166/nh.2008.034

infiltrometers, these methods do not give information about the lateral and vertical continuity of macropores (Cameira *et al.* 2000).

Mathematical models for preferential flow and transport based on different approaches have been developed during recent decades (Simunek *et al.* 2003; Gerke 2006). So-called dual porosity/permeability models are commonly used in describing the non-uniform flow in macroporous soil (Hoogmoed & Bouma 1980; Beven & Germann 1981; Ruan & Illangasekare 1998; Vogel *et al.* 2000; Cameira *et al.* 2000; Jarvis & Larsson 2001). In these models the water movement in the soil matrix is described by the Richards equation. Gerke & Van Genuchten 1993 also calculated flow in the macropore domain with the Richards equation using a different parameterization of water retention characteristics. Jarvis (1994) considered water movement in macropores as gravity flow with the hydraulic conductivity function from Germann & Beven (1985). Other descriptions of macropore flow are presented in Workman & Skaggs (1990) and Chen &Wagenet (1992).

Most of the models coupling macropore and micropore flow are one-dimensional, i.e. they describe the vertical flow of water. The models combine soil-water-atmosphere-vegetation processes such as interception, evaporation from the soil and canopy, transpiration, infiltration into soil matrix and macropores, Darcian movement of water in the matrix, rapid flow in the macropores and the exchange between these two domains. Application of a one-dimensional model is questionable on hillslopes where lateral surface and subsurface flow processes play a significant role (Smettem *et al.* 1991; Villhoth *et al.* 1998). Lateral flows are usually neglected in modelling efforts for two reasons: (1) there are only a few available two-dimensional models describing macropore flow (e.g. Bronstert & Plate 1997; Simunek *et al.* 2003; Gardenas *et al.* 2006) and (2) the data requirements of these models are extensive. Despite their limitations, one-dimensional models have remained in use also in areas of undulating topography. This study was motivated by a need to identify processes and variables that are most influenced when a sloping terrain is simplified into a one-dimensional system.

The objective of this study was to gain better understanding of the role of macroporosity in runoff generation in a sloping agricultural clayey field. Available field data indicate that soil properties vary as a function of depth and between different locations within a sloping field. In the model application the influence of these differences on hydrological variables is examined. Data for the model application were from extensive laboratory and field measurements in Southern Finland (Alakukku *et al.* 2003). Earlier measurements of drain flow, surface runoff and nutrient concentrations have given clear evidence of the occurrence of preferential flow on this experimental field (Al-Soufi 1999; Paasonen-Kivekas *et al.* 1999). The present study is aimed at quantifying macropore flow in more detail by combining the earlier measurements with a recent soil structure dataset (Alakukku *et al.* 2003; Nuutinen *et al.* 2001).

MATERIAL AND METHODS

Site description and hydrometeorological data

The measurements were conducted on a sloping field section in Sjokulla in Southern Finland (60°15′ N, 24°27′ E). Climate is temperate with mean annual precipitation of 700 mm and mean annual temperature of 5°C. The soil is classified as a very fine Aeric Cryaquept (Soil Survey Staff 1998; Peltovuori *et al.* 2002). The topsoil layer (0–0.2 m) has a clay content of 40–70% and deeper layers of 60–80%. The main clay mineral is illite, which is prone to cracking and swelling. The slope of the field varies from 2 to 4%, the upper part of the field being steeper than the lower part. Subsurface drains were installed in the early 1950s at a depth of 0.7–1.5 m with a spacing of about 13 m. Locations of the drain tiles are presented in Figure 1. The field has been mainly under spring cereal cultivation and it has been either ploughed (to a depth of 0.23–0.25 m) or stubble cultivated (to a depth of 0.15 m) in autumn. The soil was harrowed for seedbed preparation in the spring to a depth of 0.05 m.

To determine the outflow from the subsurface drain, water level was measured with a pressure sensor in front of a v-notch weir that was installed in a chamber connected to the collector pipe. Surface runoff was measured at the lowest point of the field section also by using a v-notch weir and a pressure sensor. Subsurface drain flow weir S3 (Figure 1) drained an area of 3.14 ha and the surface runoff weir P2 an area of 0.63 ha. The runoff measurements used in the current

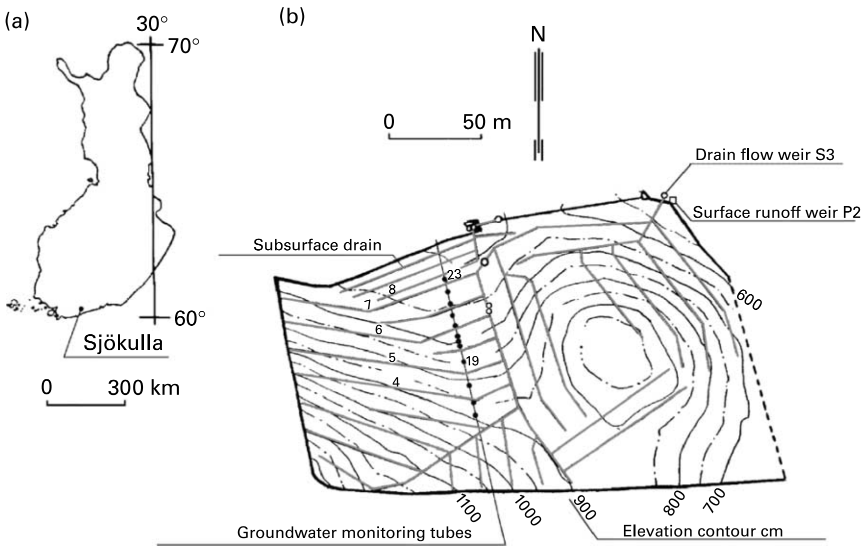

Figure 1 | Location of Sjökulla experimental field (a), and field layout of drainage network, groundwater monitoring tubes and surface runoff (P2) and subsurface drainage (S3) measurement weirs (b).

study were from 1998, which was a wet year with a number of successfully recorded precipitation-runoff events. The measurement frequency was 15 min. Along the slope shown in Figure 1 there were 12 observation tubes for groundwater level monitoring. Four of the tubes were instrumented with pressure sensors. A micrometeorological station recorded precipitation, air temperature, relative humidity, solar radiation and wind speed on site using a 15 min frequency.

Soil physical data

Soil water retention curves were determined from soil samples at the laboratory by Kankaanranta (1996) and the rest of the soil physical data were gathered in a field campaign in autumn 2001. The soil samples (0.03 m long cylinder with a diameter of 0.05 m) for analysing water retention characteristics had been taken in different field sections at three depths: 0.05–0.10 m, 0.35–0.40 m and 0.65–0.70 m. During the field campaign in 2001, the soil was sampled extensively (Figure 2). The aim of the measurements was to determine the spatial variability of soil hydraulic properties in relation to the location of a tile drain and in relation to the elevation within the field section. The samples were taken systematically along each tile drain, here referred to as *tile lines* (see Figure 2). Each tile line included 2–5 *locations,* and in each location core samples were taken at three different *points.* Point A lay just above the drain tile, point B two metres away from the tile and point C halfway between two adjacent tiles. Alakukku *et al.* (2003) have studied how macroporosity varies at different distances from the drain.

For determining macroporosity and the hydraulic conductivity of the soil, undisturbed core samples (0.55 m long PVC pipe with a diameter of 0.15 m) were taken with a tractor-driven soil auger (Poyhonen *et al.* 1997) at 52 points on the field. The core samples were cut into three subsamples: plough layer (0–0.23 m), middle layer (0.23–0.38 m) and bottom layer (the rest of the core sample). For the determination of saturated hydraulic conductivity and macroporosity the cut surfaces of the subsamples were vacuumed to expose the pores in the surface. The number of cylindrical macropores (diameter $>$ 2 mm) in the prepared surface was computed by visual inspection. The saturated hydraulic conductivity of the subsamples was determined by the constant head method, and the macroporosity (diameter $>$ 0.30–0.45 mm) was estimated by determining the volume of water extracted from a saturated soil sample at a water potential of -1.0 to -0.75 kPa, as described by Aura (1995) and Alakukku (1996).

Table 1 presents the measured mean, median, minimum and maximum values of macropore hydraulic conductivity and macroporosity in the sampling locations along five

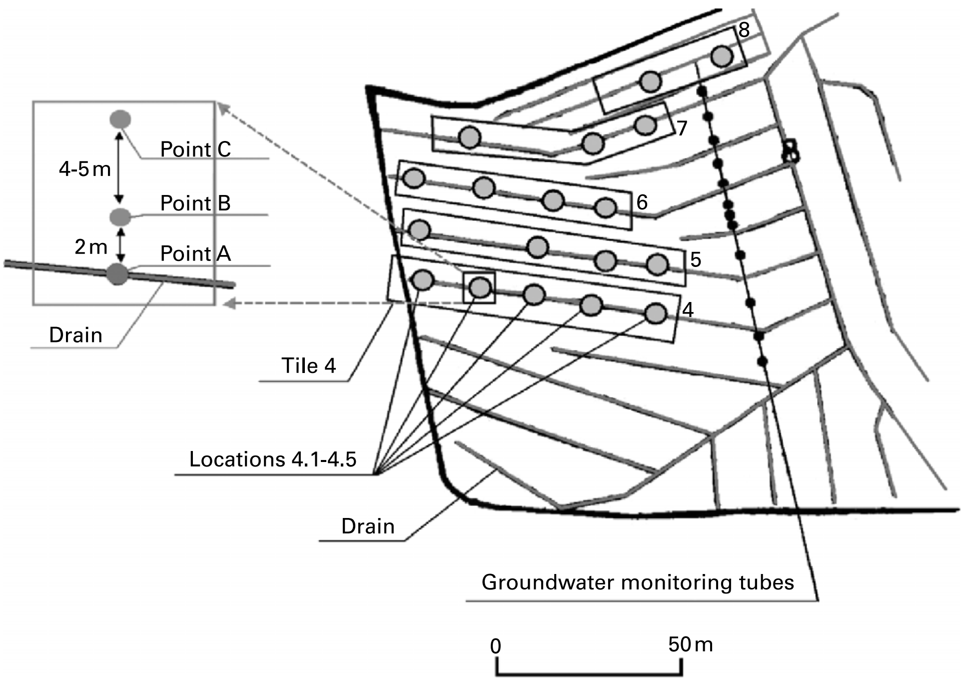

Figure 2 | Illustration of soil sampling within the field section. Each drain tile line was divided into 2–5 locations. The locations were subdivided into sampling points, and at each point a core sample was taken. Point A lay above the drain tile, point B two meters away from the tile and point C halfway between two tile lines.

different tile lines (see Figure 2). Measurement points A–C from the locations along each tile line are aggregated together in Table 1. In addition to these data, vertical profiles of moisture contents at wilting point (20 core samples) and clay contents (18 core samples) were analysed in the laboratory. Finally, in order to estimate cracking and rooting depths the soil was excavated at a few points when the crop was tillering and the root depth was expected to reach its maximum.

MACRO model

The process of soil water movement and runoff generation was modeled using MACRO, a one-dimensional physically based model developed by Jarvis (1994). Jarvis & Larsson (2001) provide documentation of the MACRO (Version 4.3) model. The model describes non-steady water flow and solute transport in macroporous soils and it accounts for plant canopy interception, vertical saturated and unsaturated flow, losses to drainage systems, evaporation from soil and root water uptake. MACRO is a dual-permeability model, where the total porosity is divided into micropores (soil matrix) and macropores. The two pore regions act as separate but interacting flow domains with their own conductivities, flow rates and solute concentrations. The driving variables given by the user are measured hourly rainfall, daily maximum and minimum air temperatures, daily wind speed, daily vapor pressure and daily global radiation.

In MACRO the partition of the pore system to micro- and macropores is defined by boundary soil water pressure head ψ_b and the corresponding water content θ_b and hydraulic conductivity K_b. The flow domains are characterized by a degree of saturation, conductivity and flux.

The vertical flow in the micropores is calculated by the Richards equation:

$$\frac{\partial \theta}{\partial t} = -\frac{\partial}{\partial z}\left[K\left(\frac{\partial \psi}{\partial z}+1\right)\right] - S_r \pm S_w \qquad (1)$$

where θ is the water content, t is the time, z is the vertical distance, K is the hydraulic conductivity, Ψ is the soil water potential, S_r is the root water uptake and S_w accounts for the water exchange between micro- and macropores.

Table 1 | Measured mean, median, minimum and maximum values of saturated hydraulic conductivity of macropores $K_{s(ma)}$ and macroporosity for the soil samples taken along five different drain tile lines (numbers from 4–8)

		$K_{s(ma)}$ mm/h			Macroporosity %		
	Layer (m)	**0–0.23**	**0.23–0.38**	**0.38–0.50**	**0–0.23**	**0.23–0.38**	**0.38–0.50**
Tile 4	Mean	151	11	0.05	3.5	0.6	0.2
	Median	119	0.07	0.04	3.4	0.4	0.2
	Min–Max	9–545	0–143	0.006–0.25	1.7–5.8	0.03–1.7	0.1–0.4
Tile 5	Mean	165	125	0.06	3.0	0.5	0.3
	Median	67	28	0.04	3.1	0.5	0.2
	Min–Max	2–1005	0.02–462	0.005–0.24	1.8–4.1	0.1–0.9	0.1–0.5
Tile 6	Mean	212	97	21	2.7	0.6	0.4
	Median	155	43	0.07	2.5	0.5	0.2
	Min–Max	26–607	0.004–306	0.01–246	1.3–4.3	0.2–2.2	0.1–2.5
Tile 7	Mean	111	115	31	2.6	0.7	0.3
	Median	38	10	0.06	2.4	0.5	0.3
	Min–Max	1–498	0.04–491	0.02–206	1.8–3.8	0.1–2.0	0.1–0.6
Tile 8	Mean	21	1	7.19	2.3	0.4	0.4
	Median	14	0.3	0.09	2.3	0.4	0.4
	Min–Max	4–52	0.04–5.2	0–29	0.5–5.4	0.2–0.6	0.2–0.7

In the soil matrix, the soil water retention characteristic $\Psi(\theta)$ is given by the Brooks & Corey (1964) function:

$$\psi_{mi} = \psi_b S_{mi}^{-1/\lambda} \tag{2}$$

where S_{mi} is the effective saturation in the micropores and λ is the pore size distribution index in the micropores.

The hydraulic conductivity of soil matrix (K_{mi}) is described by the Mualem (1976) model. Water flow in the macropores is regarded as a non-capillary, gravity-driven process and the hydraulic conductivity of macropores (K_{ma}) is expressed as a simple power law function of the degree of saturation:

$$K = K_b S_{mi}^{n+2+2/\lambda} \tag{3}$$

$$K_{ma} = K_{s(ma)} S_{ma}^{n^*} \tag{4}$$

where S_{mi} and S_{ma} are the effective saturations in the two flow regions, n is the tortuosity factor of the micropores, n^* is an empirical exponent accounting for pore size distribution in the macropores and $K_{s(ma)}$ is the saturated hydraulic conductivity of the macropores. The model accounts for the shrinkage and swelling characteristics of the soil, which alter macroporosity, microporosity and saturated hydraulic conductivity of the two pore domains (Messing & Jarvis 1990).

Lateral water exchange (S_w) between micro- and macropores is represented by an approximate solution of a reduced form of the Richards equation:

$$S_w = \left(\frac{3D_w \gamma_w}{d^2}\right)(\theta_b - \theta_{mi}) \tag{5}$$

where D_w is the effective water diffusivity, θ_{mi} is the micropore water content, γ_w is a scaling factor and d is the effective diffusion path length.

Drainflow is included as a sink term in the flow description for both micropores and macropores. Drainage flow rates from all saturated layers above the drain depth are computed by the use of seepage potential theory (Youngs 1980; Leeds-Harrison et al. 1986) and drainage flow below the drain depth is derived from the Hooghoudt equation (see Jarvis & Larsson 2001).

Potential evapotranspiration is calculated using the Penman-Monteith equation and root water uptake is calculated as a function of the evaporative demand, soil water content and root distribution. The water uptake can occur in both domains, but water is preferentially extracted from the macropores. In the current application the bottom boundary condition is such that flow out of the profile is a linear function of the water table level. At the surface boundary, the infiltrating water is partitioned between micropores and macropores, depending on the infiltration capacity of the micropores and the net rainfall intensity. Shrinkage and swelling of the clay soil and their effects on the macropore conductivity are also taken into account in the model.

Model parameterization

The data were examined in order to identify systematic spatial differences at different depths across the field. Figure 3 shows average clay contents, macroporosity and saturated hydraulic conductivity of macropores in the vicinity of each tile line (measurement points A, B and C aggregated together, see Figure 2). Data clearly indicate that macroporosity and conductivity decreased as a function of depth. The decrease of both macroporosity and saturated hydraulic conductivity with depth is a common feature in many soils (e.g. Aura 1995; Alakukku 1996). When comparing the tile lines with one another, the clearest differences were found in the clay content of the soil. Downslope by tile lines 7 and 8 the topsoil appeared to be richer in clay whereas the bottom layers (below 0.5 m) had distinctively lower values than the upper parts of the field. This is reflected also in the saturated hydraulic conductivities, topsoil of tile lines 7 and 8 being less conductive than the topsoil of tile lines 4, 5 or 6 It should be addressed that the spatial variability of the saturated hydraulic conductivity was high and few high values of conductivity had a large effect on the calculated mean of a single layer. Vertical profile of macroporosity (Figure 3(b)) was similar in all the tile lines. The data were also regrouped and averaged along lines perpendicular to the drain tile lines 4 – 7 but no systematic differences within the field were detected across the slope.

Spatial data on soil structure suggested that the hydraulic properties of the soil in the upper parts of the field differed from those in the lower parts. The idea behind the model application was to explore how such a difference is reflected in modeled runoff generation. Five separate parameterizations were formed for the MACRO model, each representing one tile line (see Figure 2). In each of these tile lines water balance and runoff generation was simulated in a vertical one-dimensional soil column. Parameter values were fixed, preferably using available field measurements. Those parameter values that could not be derived from the field data were adopted from an earlier parameterization (Hintikka 2003) or from the literature (Larsson 1999; Jarvis & Larsson 2001).

In all parameterizations the depth of the soil column was set to 2.75 m and the column was subdivided into 22 computational nodes (see Figure 4(a) as an example). The drains were set at the depths of 1.15, 1.10, 1.05, 1.0 and 0.95 m for the tile lines 4, 5, 6, 7 and 8, respectively. Macroporosities and saturated hydraulic conductivities of macropores were determined on the basis of averaged site-specific data (Table 1). In each of the three soil layers the mean measured values determined the conductivity and macroporosity of all computation nodes located within the layer. The saturated hydraulic conductivity below the depth of the soil sample core was set to a value of 0.05 mm/h in all tile lines.

The water retention characteristics were measured at only a few points on the field, and thus there were no data available separately for each site. The parameters of the soil water retention curves were estimated in two stages. First the

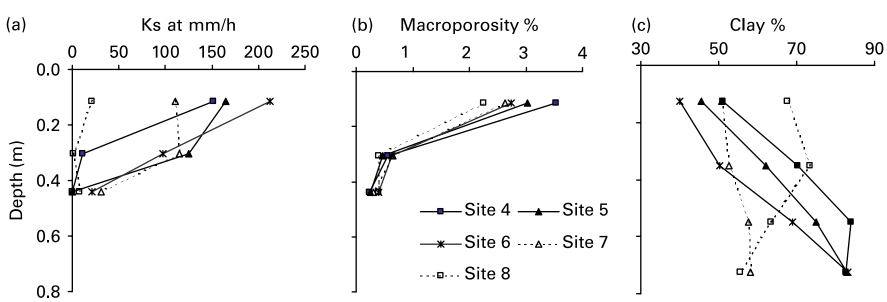

Figure 3 | Average saturated hydraulic conductivity of macropores (a), average macroporosity (>0.5 mm) (b) and average clay content (c) at different depths for each tile line. Average value for one tile line includes all measurements from points A, B and C residing along the tile line (see Figure 2).

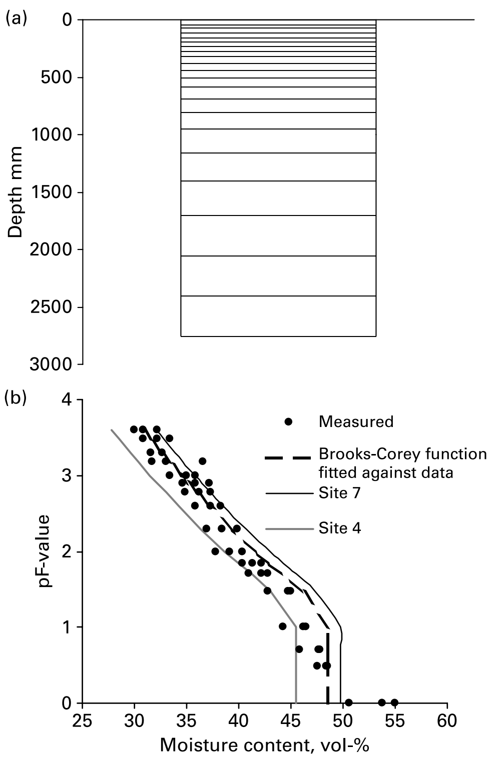

Figure 4 | Discretization of a soil column (a) and examples of water retention curves in the topsoil layer (plough layer) for tile lines 4 and 7 (b).

Brooks-Corey parameters (Equation (2)) were calibrated against the measured range of water retention curves at three different depths (0.05–0.10 m, 0.35–0.40 m and 0.65–0.70 m). The boundary soil water pressure head (ψ_b) was set to a value of -0.16 m, which indicates that pores with a radius greater than 0.2 mm are considered as macropores. In the second stage, water retention curves for tile lines 4–8 were determined. Saturated water content of micropores was estimated as a difference between measured, site-specific total porosity and macroporosity. Based on a difference between micropore saturated water content at a tile line and the saturated water content of the pF data, the values of θb and θr were shifted. An example of water retention curves for tile lines 4 and 7 in the plough layer can be seen in Figure 4(b).

The rest of the parameters were identical for all tile lines. The boundary hydraulic conductivity (K_b) was set to 0.3 mm/h in the plough layer, 0.05 mm/h in the middle layer and 0.01 mm/h below the middle layer, following Hintikka (2003). Wilting point and bulk density values were obtained from laboratory analyses and for other soil parameters default values of the model (Jarvis & Larsson 2001) were used. Crop parameters characterized typical values for cereals in Southern Finland (Karvonen 2003) or they were taken from the literature (Larsson 1999).

The simulation period started after the spring snowmelt (1 May 1998) and covered the entire growing season until the end of October 1998. This period was wet with a total precipitation of 549 mm, which was about 150 mm more than the long-term average. The initial conditions of the simulations were determined by running the model from the beginning of January to the end of April 1998.

RESULTS AND DISCUSSION

Simulation results

The MACRO model was run with the five parameterizations described in the previous section. The model results from the simulations were compared in order to identify how observed changes in soil structure affected hydrological variables.

Table 2 presents cumulative water balance components for all parameterizations. Simulated total runoff and evapotranspiration show differences between the five model set-ups, but the relative magnitude of the differences is small (less than 5% from total precipitation). Table 3 show that the small difference in evapotranspiration was only seen in the soil evaporation component, whereas transpiration and evaporation of intercepted water were not affected by the change of parameterization.

According to Table 4, the most notable difference between the simulations can be seen in the relative proportion of surface runoff and subsurface drain flow components. The largest differences in the simulated proportions of surface runoff are seen between tile lines 4, 8 and 5–7. The three tile lines 5–7 behave in a similar manner in terms of computed drain flow and surface runoff. Figure 5 shows the cumulative total runoff, surface runoff and drain flow for tile lines 4, 7 and 8. The cumulative curves indicate that the proportion of surface runoff is systematically higher and drain flow lower at tile lines 8 and 4 compared with tile line 7. Examination of Figures 3 (a) and 5 reveals that the vertical profile of macropore hydraulic conductivity has an important role in the generation of surface runoff. The profiles (tile lines 5–7) with high hydraulic conductivity (100–200 mm/h) in the two

Table 2 | Water balance components (mm/yr) for tile lines 4–8 in 1998

	Corrected precipitation	Evapotranspiration	Storage change	Percolation	Total runoff
Site 4	603.9	367.0	16.3	38.2	181.5
Site 5	603.9	357.6	12.3	36.5	196.4
Site 6	603.9	357.0	12.6	36.9	196.3
Site 7	603.9	358.9	11.5	36.6	195.8
Site 8	603.9	367.5	17.2	38.8	179.2

Table 3 | Components of evapotranspiration (mm/yr) for tile lines 4–8 in 1998

	Evapotranspiration	Transpiration	Soil evaporation	Interception
Site 4	366.9	111.1	180.4	75.5
Site 5	357.6	111.1	171.0	75.5
Site 6	357.0	111.1	170.5	75.5
Site 7	358.9	111.1	172.4	75.5
Site 8	367.5	110.4	181.7	75.5
Potential	398.5	111.1	249.7	

uppermost layers result in a generation of high cumulative volume of drain flow. The drain flow is lower at site 4, which has a low hydraulic conductivity at the depth of 0.3 m. The drain flow is the lowest (and the surface runoff the highest) at tile line 8, where the hydraulic conductivity of macropores is low throughout the profile.

The role of macropores in drain flow generation appears to be dominant in the study sites: 96–99% of modeled total drain flow was a result of preferential flow through macropores. Paasonen-Kivekas *et al.* (1999) and Al-Soufi (1999) reported that measured drainage flow in Sjokulla had a flashy response to rain storms and that nitrate concentration of drainage water after fertilizer application resembled soil water concentrations near the soil surface. These earlier findings are in line with the model results, which suggest that preferential flow has a major role in the generation of drainage flow.

The most obvious difference between simulated hourly drain flows (Figure 6(a)) is seen in the flow peaks. The height of the peaks was controlled by the maximum flow capacity of the macropores in the soil column. The macropore flow capacity at tile line 8 is lower than the capacity of lines 4 and 7 because of the less conductive soil layers. Examination of the hourly time series of surface runoff (Figure 6(b)) shows that runoff peaks were higher and were initiated earlier at tile line 8 than at line 7, which was the tile line that differed the most from line 8. During rainfall the poorly conductive soil at site 8 leads to a rapid saturation of the soil matrix and macropores, which explains the earlier occurrence and the higher peak levels of surface runoff.

Recall that in all simulations the bottom boundary condition related the flow out of the column linearly to the groundwater level. Cumulative percolation in all runs was 37–39 mm/yr with similar temporal variations (see Table 2).

Comparison with measurements

In addition to comparisons between the simulations, the results were viewed in relation to measured drain flow, surface

Table 4 | Drain flow (DF, mm/yr), surface runoff (SR, mm/yr) and their proportions for tile lines 4–8 in 1998

	Drain flow	Surface runoff	Fraction DF/Total	Fraction SR/Total
Site 4	109.2	72.3	0.60	0.40
Site 5	167.6	28.9	0.85	0.15
Site 6	169.5	26.7	0.86	0.14
Site 7	169.4	26.4	0.87	0.13
Site 8	48.5	130.7	0.27	0.73

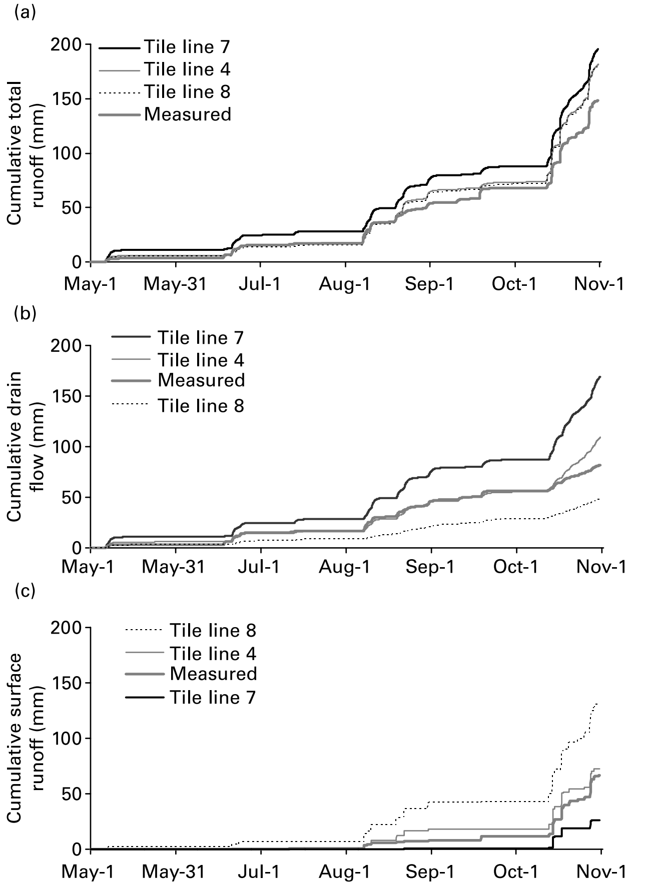

Figure 5 | The cumulative measured and simulated total runoff (a), drain flow (b) and surface runoff (c) for tile lines 4, 7, and 8 during 1998.

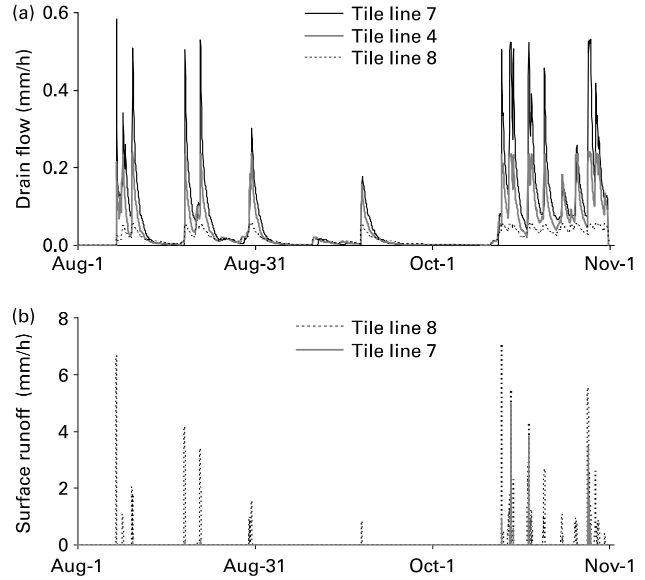

Figure 6 | Simulated hourly subsurface drain flow for lines 4, 7 and 8 (a) and simulated hourly surface runoff for lines 7 and 8 (b) during 1998.

runoff and water table level. It should be pointed out that the model was not calibrated against the measurements, because the measurements described average behavior of the field section whereas the model was parameterized separately for different locations of the field section.

According to measurements the cumulative subsurface drain flow from the entire field section was 55% of the total runoff. This percentage falls between the values from the model simulations (Table 4), although the total runoff was overpredicted in the simulations as seen in Figure 5(a). Calibrating one or more empirical model parameters such as those controlling percolation would probably decrease this error.

When compared with measurements, the model parameterization for tile line 7 tended to overestimate and the parameterization for line 8 tended to underestimate the drain flow peaks during the summer (Figures 6(a) and 7(a)). The results for tile line 4 were closer to the measurements, although the highest measured peak flows during summer were underestimated. According to these results most of the measured drain flow peaks are within the simulated minimum and maximum peak flow magnitudes. The most notable difference between the simulations and the measurements is that the simulated flow peaks are at the same level both during the summer and autumn, whereas the measured flow peaks are higher during the summer than during the autumn. Temporal change of soil structure, caused by shrinkage and swelling or soil management, is one explanation for the observed differences between the summer and autumn peak flow levels. The effect of shrinkage and cracking was accounted for in MACRO but switching off the shrinkage option showed that cracks had no effect on the simulated runoff. When simulating the wet year of 1998 the profile was never dry enough to cause substantial cracking of the soil. In autumn, after the field was ploughed and a series of rainfall events occurred consecutively, the measured drain flow peaks were lower than the modeled peaks for tile lines 4–7. Ploughing was ignored in the simulations although it can be expected to diminish the continuity of macropores (Beven & Germann 1982; Kladivko 2001).

Figure 7(b) indicates that the measured surface runoff peaks were much higher than the measured drain flow peaks

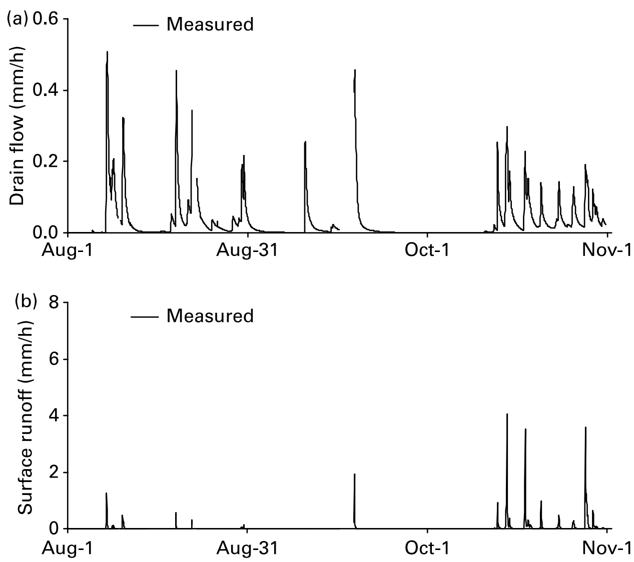

Figure 7 | Measured hourly subsurface drain flow (a) and surface runoff (b) during 1998.

and occurred mostly during the autumn. The model result in Figure 6(b) for tile line 7 resembled the measurements, whereas the surface runoff peaks for tile line 8 were higher than the measured peaks.

Comparison of the measured and modeled surface runoff hydrographs revealed that the shape of the simulated hydrographs differed from the observed hydrographs. An example of this is presented in Figure 8. The measured surface runoff events had recessions lasting several hours whereas the model simulated much more abrupt runoff responses lasting only a few hours till the end of the precipitation event. This difference is likely to be a result of lateral flow at the field surface. Surface runoff measured at the lowest point of a field comes with a lag as runoff is accumulated along the slope (see, for example, Koivusalo & Karvonen 1995). In a one-dimensional model like MACRO the surface runoff is generated when excess water ponding on the soil surface is discharged out of the system during one computational time step. Lateral surface runoff in clay hillslopes often occurs as subsurface flow through the topsoil plough layer (Aura 1990; Heppel et al. 2000). In an earlier study Al-Soufi (1999) suggested that in Sjokulla water flows laterally in macropores and cracks in the top 30 cm of the soil. As this subsurface water then reaches the lower parts of the field, it either infiltrates and contributes to the soil water storage and drain flow, or generates surface runoff. Occurrence of lateral subsurface flow in the plough layer could not be accounted for in the current model.

Simulated groundwater levels by the parameterizations for tile lines 4 and 7 are shown in Figure 9 together with measurements conducted in the vicinity of the tile lines (see Figure 2). Examination of groundwater levels revealed that groundwater rose slightly more quickly in response to rainfall events at site 4 than at site 7. Smaller macroporosity in the subsoil of site 4 explains this behavior. In autumn, the groundwater table at site 4 was drawn down slower than at site 7, but in summertime the decrease in the water table was slightly more rapid. The slow dissipation of the water table in the autumn was due to the lower flow capacity of macropores and its effect on drain flow. During the summer the difference in drawdown of groundwater table was again caused by lower macroporosity at site 4. In the model, water demand by crops was preferentially satisfied from water stored in the macropores. Since macroporosity was lower beneath

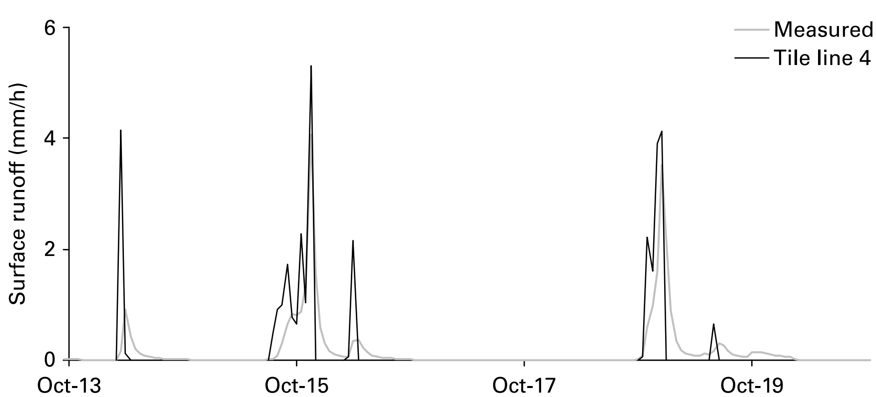

Figure 8 | Measured and simulated (tile line 4) hourly surface runoff during 13–20 October 1998.

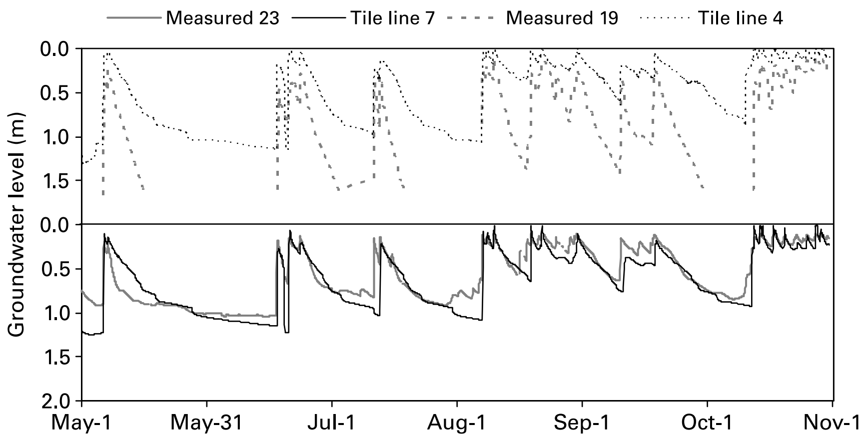

Figure 9 | Simulated depths to groundwater table at tile lines 4 and 7 and measured depths in nearby groundwater monitoring tubes 23 and 19 (see Figure 1) during 1998. Missing values of measured depth to groundwater table in tube 23 are due to water table sinking below the measurement range of a pressure sensor.

the topsoil of site 4, roots emptied the macropores more rapidly and started earlier to extract water stored in micropores.

The simulated groundwater levels at site 7 matched well the observed groundwater table dynamics at tube 23 but the outcome of site 4 was poor (Figure 9). The measured water levels suggest that the hydraulic gradient between upslope and downslope areas generated lateral groundwater flow. Connection between upper and lower parts of the field through groundwater flow was not accounted for in the current simulations. Using dissimilar bottom boundary conditions for each parameterization could be one possibility to account for lateral groundwater flow. However, as long as the models for the upper and lower parts are not coupled together, i.e. solved simultaneously, lateral groundwater flow cannot be described without calibrating the two models separately. For example, additional test runs (not shown here) indicated that simulation results at site 4 in terms of reproducing groundwater level and total runoff were improved, when the parameter controlling percolation was calibrated. Yet the proportional fractions of drain flow and surface runoff were insensitive to the calibration of the percolation parameter.

When the model results are compared with the measurements, one can evaluate when it is necessary to use a multidimensional approach in characterizing the hydrology of a sloping subsurface drained field. The current results suggest that the one-dimensional model can be applied to quantify average water balance and total runoff response on a clay hillslope. A two-dimensional model becomes advisable when prediction of proportional fractions of drain flow and surface runoff is important. Also the short-term prediction of surface runoff and simulation of internal processes within the field, such as groundwater levels, necessitate a description of water movement in two or three dimensions. Consideration of the spatial variability of soil structure and its effects on runoff components would aid in achieving a more realistic prediction of sediment and nutrient transport in clay soils.

CONCLUSIONS

Field data indicated that soil structure varied with respect to the depth from the soil surface and between upslope and downslope areas within the field. The difference in macropore conductivity between topsoil and subsoil was greater in the upper parts of the field than in the downslope area.

Based on the measured differences in soil structure five separate model parameterizations were implemented in order to simulate how the soil structure affects the hydrological response of a clay field. Changing soil parameterization had the greatest effect on the relative proportions of drain flow and surface runoff. However, the total amount of runoff was only slightly affected. Evapotranspiration and percolation were not sensitive to differences in soil structure.

The results suggested that a one-dimensional model was sufficient to quantify average water balance and total runoff response on a sloping clay field. Use of a two-dimensional approach becomes advisable when prediction of proportional fractions of drain flow and surface runoff are of interest. In addition, realistic simulation of surface runoff hydrographs and spatially variable internal processes within the field call for a two- or three- dimensional approach.

ACKNOWLEDGEMENTS

This study was funded by the Finnish Drainage Research Foundation, the Ministry of Agriculture and Forestry and the Land and Water Technology Foundation (Maa- ja vesitekniikan tuki ry). We are grateful to Prof. Tuomo Karvonen, Prof. Pertti Vakkilainen and Dr. Mark Gill for valuable comments and support. Special thanks are due to Mrs. Marja-Liisa Westerlund, Mr. Taisto Siren, Mr. Leo Tirkkonen, Mr. Matti Ylösmäki and Mr. Antti Ristolainen for carrying out soil sampling and measurements.

REFERENCES

Alakukku, L. 1996 Persistence of soil compaction due to high axle load traffic. II. Long-term effects on the properties of fine-textured and organic soils. *Soil Till. Res.* **37**, 223–238.

Alakukku, L. 1998 Properties of compacted fine-textured soils as affected by crop rotation and reduced tillage. *Soil Till. Res.* **47**, 83–89.

Alakukku, L., Nuutinen, V., Koivusalo, H. & Paasonen-Kivekas, M. 2003 Macroporosity of three arable clays in relation to subdrain location. In: *ISTRO 16th Triennial Conference: Soil Management for Sustainability, University of Queensland, Brisbane, Australia, 14–18 July*. International Soil Tillage Research Organisation (ISTRO), pp 16–22.

Al-Soufi, R. 1999 *Analysis of Macropore Flow in Sjökulla Research Field*. Helsinki University of Technology, Publications of the Water Resources Laboratory, Otaniemi.

Aura, E. 1990 *Subsurface Drainage in Finnish Heavy Clay Soils* (in Finnish: *Salaojien toimivuus savimaassa*). Maatalouden tutkimuskeskus, Jokioinen, Tiedote 10/90.

Aura, E. 1995 Finite element modelling of subsurface drainage in Finnish heavy clay soils. *Agric. Wat. Mngmnt.* **28**, 35–47.

Beven, K. & Germann, P. 1981 Water flow in macropores II. A combined flow model. *Soil Sci.* **32**, 15–29.

Beven, K. & Germann, P. 1982 Macropores and water flow in soils. *Wat. Res. Res.* **18**, 1311–1325.

Bronstert, A. & Plate, E. J. 1997 Modelling of runoff generation and soil moisture dynamics for hillslopes and micro-catchments. *J.Hydrol.* **198**, 177–195.

Brooks, R. H. & Corey, A. T. 1964 *Hydraulic Properties of Porous Media*. Colorado State University, Fort Collins, CO, Paper no.3.

Cameira, M. R., Ahuja, L., Fernando, R. M. & Pereira, L. S. 2000 Evaluating field measured soil hydraulic properties in water transport simulations using the RZWQM. *J. Hydrol.* **236**, 78–90.

Chen, C. & Wagenet, R. J. 1992 Simulation of water and chemicals in macropore soils, I, Representation of the equivalent macropore influence and its effect on soil-water flow. *J. Hydrol.* **130**, 105–126.

Fox, G. A., Malone, R., Sabbagh, G. J. & Rojas, K. 2004 Interrelationship of macropores and subsurface drainage for conservative tracer and pesticide transport. *J. Environ. Qual.* **33**, 2281–2289.

Gärdenäs, A., Šimůnek, J., Jarvis, N. & Van Genuchten, M. Th. 2006 Two-dimensional modelling of preferential water flow and pesticide transport from a tile-drained field. *J. Hydrol.* **329**, 647–660.

Gerke, H. H. 2006 Review article: preferential flow descriptions for structured soils. *J. Plant Nutr. Soil Sci.* **169**, 382–400.

Gerke, H. H. & Van Genuchten, M. T. 1993 A dual-porosity model for simulating the preferential movement of water and solutes in structured porous media. *Wat. Resour. Res.* **29**, 305–319.

Germann, P. & Beven, K. 1985 Kinematic wave approximation to infiltration into soils with sorbing macropores. *Wat. Resour. Res.* **21**, 990–996.

Heppel, C. M., Burt, T. P. & Williams, R. J. 2000 Variations in the hydrology of an underdrained clay hillslope. *J. Hydrol.* **227**, 236–256.

Hintikka, S. 2003 *Effect of Macroporosity on Drain Flow and Surface Runoff in Clay Soils* (in Finnish: *Makrohuokoston vaikutus pinta-ja salaojavaluntaan savimailla)*. Master's thesis,Laboratory of Water Resources, Helsinki University of Technology.

Hoogmoed, W. B. & Bouma, J. 1980 A simulation model for predicting Infiltration into cracked clay soil. *Soil Sci. Soc. Am. J.* **44**, 458–461.

Jarvis, N. J. 1994 *The MACRO Model (Version 3.1). Technical Description and Sample Simulations*. Department of Soil Science, Swedish University of Agricultural Sciences, Uppsala, Sweden, Reports and Dissertation 19.

Jarvis, N. J. 2007 A review of non-equilibrium water flow and solute transport in soil macropores: principles, controlling factors and consequences for water quality. *Eur. J. Soil Sci.* **58**, 523–546.

Jarvis, N. J. & Larsson M. H. 2001 *The MACRO Model (Version 4.3). Technical Description*. Available at: http://www-mv.slu.se/bgf/Macrohtm/macro43b/TechMacro43.pdf. Accessed 21 June 2007.

Jaynes, D. B., Ahmed, S. I., Kung, K.-J. S. & Kanwar, R. S. 2001 Temporal dynamics of preferential flow to a subsurface drain. *Soil Sci. Soc. Am. J.* **65**, 1368–1376.

Kankaanranta, J. 1996 *Water Flow and Nutrient Leaching in Clay Soils* (in Finnish: *Veden virtaus ja ravinteiden huuhtoutuminen savimaassa)*. Master's thesis, Laboratory of Water Resources, Helsinki University of Technology.

Karvonen, T. 2003 *Influence of Global Climatic Change on Different Hydrological Variables*. Available at:

http://www.water.hut.fi/wr/kurssit/Yhd-12.135/kirja/paa_e.htm. Accessed 21 June 2007.

Kladivko, E. J. 2001 Tillage systems and soil ecology. *Soil Till. Res.* **61**, 61–76.

Koivusalo, H. & Karvonen, T. 1995 Modeling surface runoff – A case study of a cultivated field in Southern Finland. *Nordic Hydrol.* **26**, 205–222.

Larsson, M. 1999 *Quantifying Macropore Flow Effects on Nitrate and Pesticide Leaching in a Structured Soil. Field Experiments and Modelling with the MACRO and SOILN Models*. Agraria 164, Swedish University of Agricultural Sciences.

Leeds-Harrison, P. B., Shipway, C. J. P., Jarvis, N. J. & Youngs, E. G. 1986 The influence of soil macroporosity on water retention, transmission and drainage in a clay soil. *Soil Use Mngmnt.* **2**, 47–50.

Messing, I. & Jarvis, N. J. 1990 Seasonal variation in field-saturated hydraulic conductivity in two swelling clay soils in Sweden. *J. Soil Sci.* **41**, 229–237.

Mitchell, A.R., and Van Genuchten, M. Th 1993 Flood irrigation of a cracked soil. *Soil Sci. Soc. Am. J.* **57** 490–497.

Mualem, Y. 1976 A new model for predicting the hydraulic conductivity of unsaturated porous media. *Wat. Res. Res.* **12**, 513–522.

Novak, V., Simunek, J. & van Genuchten, M. T. 2000 Infiltration of water into soil with cracks. *J. Irrig. Drain. Engng.* **126**, 41–47.

Nuutinen, V., Pöyhönen, S., Ketoja, E. & Pitkänen, J. 2001 Abundance of the earthworm Lumbricus terrestris in relation to subsurface drainage pattern on a sandy clay field. *Eur. J. Soil Biol.* **37**, 301–304.

Paasonen-Kivekäs, M., Koivusalo, H., Karvonen, T., & Vakkilainen, P. 2000 *Nutrient Leaching on Subsurface Drained Clay Soil* (in Finnish: *Ravinteiden huuhtoutuminen salaojitetussa savimaassa*). Institute of Applied Chemistry and Microbiology, University of Helsinki, Helsinki. Pro Terra 4/2000, 92–94.

Paasonen-Kivekäs, M., Koivusalo, H., Karvonen, T., Vakkilainen, P. & Virtanen, J. 1999 Nitrogen transport via surface and subsurface flow in an agricultural field. *Proceedings of lUGG 99 Symposium HS3, Birmingham, July*. IAHS Publ. 257, IAHS, Wallingford, pp. 163–169.

Peltovuori, T., Uusitalo, R. & Kauppila, T. 2002 Phosphorus reserves and apparent phosphorus saturation in four weakly developed cultivated pedons. *Geoderma* **110**, 35–47.

Pöyhönen, A., Alakukku, L. & Pitkänen, J. 1997 *Mechanization of the Sampling of Large Soil Cores and Physical Stress of Soil Sampling* (in Finnish: *Maanäytteenoton koneellistaminen ja työntutkimus*). Maatalouden tutkimuskeskuksen julkaisuja. Sarja A, **22**, pp 1–39.

Ruan, H. & Illangasekare, T. H. 1998 A model to couple overland flow and infiltration into macroporous vadose zone. *J. Hydrol.* **210**, 116–127.

Šimůnek, J., Jarvis, N. J., Van Genuchten, M. Th. & Gärdenäs, A. 2003 Review and comparison of models for describing non-equilibrium and preferential flow and transport in the vadose zone. *J. Hydrol.* **272**, 14–35.

Smettem, K. R. J., Chittleborough, D. J., Richards, B. G. & Leaney, F. W. 1991 The influence of macropores on runoff generation from a hillslope soil with a contrasting textural class. *J. Hydrol.* **122**, 235–252.

Soil Survey Staff 1998 *Keys to Soil Taxonomy*, 8th edn. United States Department of Agriculture, Natural Resources Conservation Service. US Government Printing Office, Washington, DC.

Villhoth, K. G., Jensen, K. H. & Fredericia, J. 1998 Flow and transport processes in macroporous subsurface-drained glacial till soil. I: Field investigation. *J. Hydrol.* **207**, 98–120.

Vogel, T., Gerke, H. H., Zhang, R. & Van Genuchten, M. Th. 2000 Modeling flow and transport in a two-dimensional dual-permeability system with spatially variable hydraulic properties. *J. Hydrol.* **238**, 78–89.

Watson, K. W. & Luxmoore, R. J. 1986 Estimating macroporosity in a forest watershed by use of a tension infiltrometer. *Soil Sci. Soc. Am. J.* **50**, 578–582.

Workman, S. R. & Skaggs, R. W. 1990 PREFLO: a water management model capable of simulating preferential flow. *Trans. ASAE* **33**, 1939–1948.

Youngs, E. G. 1980 The analysis of groundwater seepage in heterogeneous soils. *Hydrol. Sci. Bull.* **25**, 155–165.

First received 15 December 2006; accepted in revised form 5 September 2007